

# The Rotational Zeeman Effect of Formylchloride

K.-F. Dössel, J. Wiese, and D. H. Sutter

Abt. Chemische Physik im Institut für Physikalische Chemie der Christian Albrechts Universität, Kiel

Z. Naturforsch. **33a**, 21–28 (1978); received November 2, 1977

The rotational Zeeman effect of several low  $J$  transitions of Formylchloride was investigated at fields close to 25 kGauss. The results are compared to those for Formylfluoride. The larger values for the paramagnetic susceptibilities are indicative for low lying excited electronic states which together with the comparatively large molecular electric quadrupole moments may be the reason for the low stability of the molecule.

## Introduction

Although Formylfluoride is a stable molecule and has been known for many years [1] it remained until 1973 [2] that first spectroscopic evidence proved the existence of its heavier homologue Formylchloride. The rotational spectrum and structural parameters of several isotopic species of HCOCl have been reported previously [3]. In the following we report the results of a rotational Zeeman-effect investigation carried out in order to get more information on the electronic structure of this unstable molecule.

## Experimental

Because of the instability of Formylchloride in the waveguide-cell, we had to use a flow system. A slow stream of HCOOH was passed through a U-tube packed with  $\text{PCl}_5$ . The gas mixture containing HCOCl and  $\text{POCl}_3$  was then lead through a trap immersed in an acetone/dry ice slush to deposit the  $\text{POCl}_3$ . The HCOCl was slowly pumped through the waveguide-cell keeping the pressure approximately at 50 mTorr. The spectra were recorded with a conventional 33 kHz square-wave Stark-effect modulated microwave spectrometer equipped with an electromagnet. Details of the design of the Zeeman-microwave-spectrometer may be found elsewhere [4, 5]. The waveguide-cell was not cooled and the observed halfintensity-halfline-widths, which are essentially due to collision-broadening, were on the order of 150 to 200 kHz. The observed shifts of the Zeeman satellites with respect to the zero-field centre-frequencies, the latter being calculated as the intensity weighted

mean [6] of all hyperfine components belonging to one rotational transition, are listed in Table 2. Although the applied Stark-fields were high enough to fully modulate the lines, interference from Stark-effects of other, nearby hyperfine components could occur. The remaining discrepancies between observed and calculated frequencies may be partly due to this effect.

## Theory

The appropriate effective Hamiltonian for a rigid-rotor molecule, containing one quadrupole nucleus and rotating in an exterior magnetic field, is given by Eq. (1) [7]

$$\begin{aligned}\mathcal{H}_{\text{eff}} &= \mathcal{H}_{\text{rot}} + \mathcal{H}_{\text{Q}} + \mathcal{H}_{\text{mag}}, \\ \mathcal{H}_{\text{mag}} &= \mathcal{H}_{\text{g}}^{\text{mol}} + \mathcal{H}_{\text{g}}^{\text{nucl}} + \mathcal{H}_{\text{z}}.\end{aligned}\quad (1)$$

$\mathcal{H}_{\text{rot}}$  is the standard zero-field rigid-rotor Hamiltonian, and  $\mathcal{H}_{\text{Q}}$  is the nuclear quadrupole interaction Hamiltonian.  $\mathcal{H}_{\text{g}}^{\text{mol}}$  and  $\mathcal{H}_{\text{g}}^{\text{nucl}}$  describe the molecular and shielded nuclear Zeeman effect and  $\mathcal{H}_{\text{z}}$  arises from the interaction between the field-induced magnetic moment and the applied magnetic field.

If the Hamiltonian matrix is set up in the uncoupled basis,  $|J, \tau, M_J, I, M_I\rangle$ , it factorizes, at least to a first approximation, into submatrices which correspond to the different rotational states and which are characterized by the rigid rotor quantum number  $J$  and  $\tau$ . Because the matrix-elements which connect these different  $J, \tau$ -submatrices (they stem from  $\mathcal{H}_{\text{mag}}$  and  $\mathcal{H}_{\text{Q}}$ ) are smaller by a factor of  $10^{-3}$  than the energy separations between the different  $J, \tau$ -blocks, they do contribute only very little to the eigenvalues of the Hamiltonian. In fact, a second order perturbation treatment showed, that their contributions to the

Sonderdruckanforderungen an Prof. Dr. D. H. Sutter, Institut für Physikalische Chemie, Christian Albrechts Universität, D-2300 Kiel.



Dieses Werk wurde im Jahr 2013 vom Verlag Zeitschrift für Naturforschung in Zusammenarbeit mit der Max-Planck-Gesellschaft zur Förderung der Wissenschaften e.V. digitalisiert und unter folgender Lizenz veröffentlicht: Creative Commons Namensnennung-Keine Bearbeitung 3.0 Deutschland Lizenz.

Zum 01.01.2015 ist eine Anpassung der Lizenzbedingungen (Entfall der Creative Commons Lizenzbedingung „Keine Bearbeitung“) beabsichtigt, um eine Nachnutzung auch im Rahmen zukünftiger wissenschaftlicher Nutzungsformen zu ermöglichen.

This work has been digitalized and published in 2013 by Verlag Zeitschrift für Naturforschung in cooperation with the Max Planck Society for the Advancement of Science under a Creative Commons Attribution-NoDerivs 3.0 Germany License.

On 01.01.2015 it is planned to change the License Conditions (the removal of the Creative Commons License condition "no derivative works"). This is to allow reuse in the area of future scientific usage.

measured Zeeman-hfs-patterns are less than 5 kHz, which is below the experimental uncertainty. We therefore neglected these matrixelements off-diagonal in  $J$  and  $\tau$  altogether, which simplified the analysis.

The nonvanishing matrixelements of the  $J, \tau$ -submatrices are listed in the appendix. With the applied fields on the order of 25 kGauss, the matrixelements of  $\mathcal{H}_g^{\text{mol}}$  and  $\mathcal{H}_g^{\text{nucl}}$ , which are diagonal in  $M_J$  and  $M_I$ , are comparable in magnitude to the matrixelements of  $\mathcal{H}_Q$ , which are both diagonal and offdiagonal in  $M_J$  and  $M_I$ . Thus mixing of different  $M_J, M_I$ -states is rather strong and  $M_J$  and  $M_I$  loose their meaning as projection quantum numbers for the rotational and spin angular momenta. However in many cases the contribution of a single  $M_J, M_I$ -state to the eigenstate is so dominant, that  $M_J$  and  $M_I$  are still usefull to assign the latter.

In order to diagonalize the different  $J\tau$ -blocks of the matrix numerically the computer routine DZQDG.F4 by E. Hamer [8] was used. This routine works as follows:

Consider a transition  $J, \tau \rightarrow J', \tau'$ . The matrix of  $\mathcal{H}_{\text{eff}}$  is first set up for the lower of the two involved rotational levels and diagonalized by an orthogonal transformation:

$$(V_l)^t \cdot (J, \tau) \cdot (V_l) = (J, \tau)_{\text{diag}} \quad (2)$$

and equally for the upper rotational level:

$$(V_u)^t \cdot (J', \tau') \cdot (V_u) = (J', \tau')_{\text{diag}}. \quad (3)$$

$(J, \tau)$  and  $(J', \tau')$  designate the  $M_J, M_I$ -submatrices corresponding to the  $J, \tau$ - and  $J', \tau'$  rotational states. They are of rank  $(2J+1)(2I+1)$  and  $(2J'+1)(2I+1)$  respectively with nuclear spin  $I=3/2$  for the Chlorine nucleus.  $(V_l)$  and  $(V_u)$  stand for the unitary transformation matrices which diagonalize  $(J, \tau)$  and  $(J', \tau')$ . They consist of the Eigenvectors of  $(J, \tau)$  and  $(J', \tau')$ . In both Equations the upper index  $t$  designates the corresponding transposed matrix.

$(V_l)$  and  $(V_u)$  are then used to calculate the relative intensities by transforming the  $M$ -dependent part of the direction cosine matrix from the uncoupled  $|J, \tau, M_J, I, M_I\rangle$  basis to the coupled basis in which  $\mathcal{H}_{\text{eff}}$  is diagonal. This is done by multiplying the cosine matrix with the transpose of the lower eigenvector matrix from the left and the upper eigenvector matrix from the right:

$$(V_l)^t \cdot (\cos(aZ)) \cdot (V_u) = (\cos(aZ)). \quad (4)$$

uncoupled basis                      coupled basis

Although the quantum numbers  $M_J$  and  $M_I$  are no longer “good” quantum numbers in the coupled basis, they were retained to characterize the observed Zeeman satellites for the following three transitions,

$$0_{00} \rightarrow 1_{01}, \quad 1_{10} \rightarrow 2_{11}, \quad 1_{11} \rightarrow 2_{12}.$$

On the other hand, due to the intermediate coupling situation at fields close to 25 kG, neither the quantum numbers of the uncoupled basis,  $M_J$  and  $M_I$ , nor those of the coupled basis,  $F$  and  $M_F$ , are

$J_{K-K+} \rightarrow J'_{K'-K'+}$	$F \rightarrow F'$	rel. int.	$\nu_{\text{obs}}$	$\Delta\nu_{\text{obs}}$	$\Delta\nu_{\text{calc}}$
$0_{00} \rightarrow 1_{01}$	3/2 5/2	50.0	11828.58		
	3/2 3/2	33.3	11815.87	12.71	12.78
	3/2 5/2	50.0	11828.58		
	3/2 1/2	16.7	11838.78	-10.20	-10.22
$1_{01} \rightarrow 2_{02}$	3/2 3/2	10.7	23660.04		
	5/2 7/2	40.0	23650.93	9.11	9.13
	3/2 3/2	10.7	23660.04		
	1/2 3/2	8.3	23637.04	23.00	23.00
	3/2 3/2	10.7	23660.04		
	5/2 5/2	9.0	23638.12	21.92	21.90
	3/2 3/2	10.7	23660.04		
$1_{11} \rightarrow 2_{12}$	1/2 1/2	8.3	23649.81	10.23	10.23
	3/2 3/2	10.7	23190.70		
	5/2 7/2	40.0	23199.74	- 9.04	- 9.04
	3/2 3/2	10.7	23190.70		
	3/2 5/2	21.0	23186.98	3.72	3.74
	3/2 3/2	10.7	23190.70		
	1/2 3/2	8.3	23204.25	-13.55	-13.59
	3/2 3/2	10.7	23190.70		
	1/2 1/2	8.3	23209.59	-18.89	-18.82

Table 1. Zero field  $^{35}\text{Cl}$ -hfs splittings of some rotational transitions in HCICO. The quadrupole coupling constants listed at the bottom of Table 3 were fitted to the observed splittings listed in the column headed by  $\Delta\nu_{\text{obs}}$ .  $\Delta\nu_{\text{calc}}$  gives the corresponding splittings calculated from the optimized coupling constants.

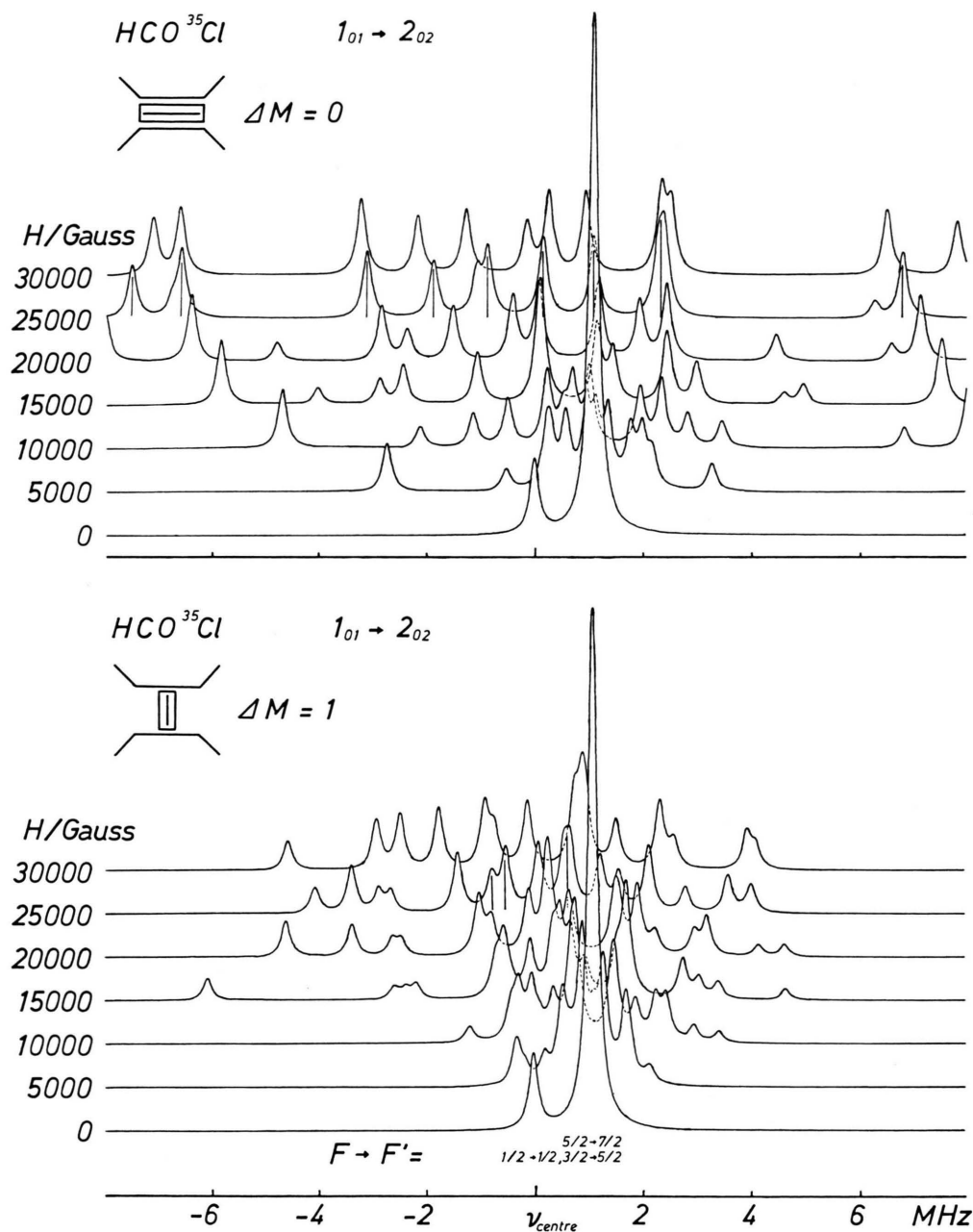


Fig. 1. Field dependence in the central region of the  $1_{01} \rightarrow 2_{02}$  rotational transition calculated from the molecular parameters listed in Table 3. At fields close to 25 kG considerable mixing of the different states either of the uncoupled (high field) or of the coupled (zero field) limiting cases occurs and neither  $M_J$  and  $M_I$  nor  $F$  and  $M_F$  are appropriate to characterize the transitions. Therefore calculated Zeeman satellites, which correspond to those observed at 25.05 kG for parallel fields (" $\Delta M_J = 0$ ") and at 23.336 kG for perpendicular fields (" $\Delta M_J = \pm 1$ "), are marked by vertical bars.

appropriate for the designation of the satellites of the  $1_{01} \rightarrow 2_{02}$  transition. For this reason we give a perspective plot of the calculated field dependence

of the central region of this transition pattern in Figure 1. The corresponding observed frequencies are listed in Table 2.

Table 2. Zeeman splittings (all frequencies given in MHz). The center frequencies  $\nu_c$  are the hypothetical frequencies of the corresponding rotational transition excluding the effect of nuclear quadrupole coupling and are calculated from a least squares fit to our data presented in Table 1. For unresolved Zeeman satellites we fitted to the intensity weighted means of the frequencies of the involved satellites. In the Table the columns headed by “Int.,” “ $\Delta\nu_{\text{calc}}$ ,” and “ $\overline{\Delta\nu_{\text{calc}}}$ ” give the corresponding intensities (arb. units), frequency shifts, and intensity weighted frequency shifts as calculated from the final Zeeman parameters listed in Table 3.

$0_{00} \rightarrow 1_{01}$			$\nu_c = 11826.04$			$\Delta M_J = 0$	$H = 25.050 \text{ kG}$
$M_I$	$M_J$	$M_J$				$\Delta\nu_{\text{obs}}$	$\Delta\nu_{\text{obs}} - \Delta\nu_{\text{calc}}$
3/2	0	0				-7.53	0.00
1/2	0	0				6.09	0.08
-1/2	0	0				2.67	0.03
-3/2	0	0				-1.87	0.04
$1_{01} \rightarrow 2_{02}$			$\nu_c = 23649.82$			$\Delta M_J = 0$	$H = 25.050 \text{ kG}$
$M_I$	$M_J$	$M_J$	Int.	$\Delta\nu_{\text{calc}}$	$\overline{\Delta\nu_{\text{calc}}}$	$\Delta\nu_{\text{obs}}$	$\Delta\nu_{\text{obs}} - \Delta\nu_{\text{calc}}$
no quantum numbers appropriate however see Fig. 1			14.4	2.40	2.34	2.35	0.01
			11.3	2.27		-0.84	0.05
						-7.54	0.00
						6.83	0.03
						-3.09	0.02
						1.13	0.02
						0.16	0.01
						-1.84	0.04
						-6.62	-0.01
$1_{10} \rightarrow 2_{11}$			$\nu_c = 24107.64$			$\Delta M_J = 0$	$H = 24.115 \text{ kG}$
$M_I$	$M_J$	$M_J$	Int.	$\Delta\nu_{\text{calc}}$	$\overline{\Delta\nu_{\text{calc}}}$	$\Delta\nu_{\text{obs}}$	$\Delta\nu_{\text{obs}} - \Delta\nu_{\text{calc}}$
3/2	-1	-1	10.5	3.00	3.03	3.13	0.10
-1/2	-1	-1	10.9	3.06			
1/2	-1	-1	10.1	3.85			
1/2	0	0	14.8	3.56	3.71	3.71	0.00
-3/2	-1	-1	11.3	3.78			
$1_{10} \rightarrow 2_{11}$			$\nu_c = 24107.64$			$\Delta M_J = 0$	$H = 25.630 \text{ kG}$
$M_I$	$M_J$	$M_J$	Int.	$\Delta\nu_{\text{calc}}$	$\overline{\Delta\nu_{\text{calc}}}$	$\Delta\nu_{\text{obs}}$	$\Delta\nu_{\text{obs}} - \Delta\nu_{\text{calc}}$
3/2	-1	-1	10.7	3.17	3.20	3.27	0.07
-1/2	-1	-1	11.0	3.23			
3/2	1	1	11.1	-4.00	-4.07	-3.91	0.16
-3/2	0	0	14.7	-4.12		3.66	0.07
1/2	0	0				3.89	-0.06
-3/2	-1	-1	10.3	3.98	3.95	-3.67	0.02
1/2	-1	-1	11.3	3.92		-3.01	-0.06
-1/2	1	1					
-3/2	1	1					
$1_{11} \rightarrow 2_{12}$			$\nu_c = 23196.75$			$\Delta M_J = 0$	$H = 25.630 \text{ kG}$
$M_I$	$M_J$	$M_J$	Int.	$\Delta\nu_{\text{calc}}$	$\overline{\Delta\nu_{\text{calc}}}$	$\Delta\nu_{\text{obs}}$	$\Delta\nu_{\text{obs}} - \Delta\nu_{\text{calc}}$
3/2	0	0				-3.73	0.16
3/2	-1	-1	10.3	4.98	5.12	5.05	-0.07
1/2	0	0	14.7	5.22		-2.87	-0.06
3/2	1	1				3.40	-0.09
1/2	0	0	14.6	3.57	3.49	-4.85	0.07
1/2	-1	-1	10.5	3.38			
-1/2	1	1	10.9	-4.81	-4.92		
-3/2	0	0	14.6	-5.01			

Table 2, continued

$1_{01} \rightarrow 2_{02}$			$v_c = 23649.82$			$\Delta M_J = \pm 1 \quad H = 23.336 \text{ kG}$	
$M_I$	$M_J$	$M_J$	Int.	$\Delta v_{\text{calc}}$	$\overline{\Delta v_{\text{calc}}}$	$\Delta v_{\text{obs}}$	$\Delta v_{\text{obs}} - \Delta v_{\text{calc}}$
no quantum numbers appropriate however see Fig. 1						-1.15	0.10
			12.0	0.17		-0.96	-0.16
			10.2	0.42	0.28	0.32	0.04
$1_{10} \rightarrow 2_{11}$			$v_c = 24107.64$			$\Delta M_J = \pm 1 \quad H = 23.336 \text{ kG}$	
$M_I$	$M_J$	$M_J$				$\Delta v_{\text{obs}}$	$\Delta v_{\text{obs}} - \Delta v_{\text{calc}}$
3/2	1	2				3.04	0.04
-3/2	1	-2				3.38	-0.09
$1_{11} \rightarrow 2_{12}$			$v_c = 23196.75$			$\Delta M_J = \pm 1 \quad H = 23.336 \text{ kG}$	
$M_I$	$M_J$	$M_J$	Int.	$\Delta v_{\text{calc}}$	$\overline{\Delta v_{\text{calc}}}$	$\Delta v_{\text{obs}}$	$\Delta v_{\text{obs}} - \Delta v_{\text{calc}}$
-1/2	0	-1				2.39	-0.01
-1/2	-1	-2	10.3	-2.03	-2.05	-2.06	-0.01
-3/2	0	-1	5.7	-2.07		3.62	-0.06
-3/2	-1	-2				1.38	0.03
-3/2	1	2					

### Assignment of Lines

We rerecorded 13 low  $J$ ,  $\mu_a$ -type hyperfine transitions (see Table 1) under field free conditions. The agreement with the frequencies given by Takeo and Matsumura [3] was moderately good, the worst deviation being 110 kHz. The rotational constants we determined are within their quoted uncertainties, but we feel, that our  $^{35}\text{Cl}$  quadrupole coupling constants are somewhat better than theirs. Our values are listed at the bottom of Table 3.

For the observation of the molecular Zeeman effect we chose the  $0_{00} \rightarrow 1_{01}$ ,  $1_{01} \rightarrow 2_{02}$ ,  $1_{01} \rightarrow 2_{11}$  and  $1_{11} \rightarrow 2_{12}$  rotational transitions. The resulting Zeeman pattern is very complicated (except for the  $0_{00} \rightarrow 1_{01}$  transition) and there are many overlapping lines. Fortunately our first guess of the molecular  $g$ -factors, which was based on the data obtained for HCOF [10, 11], came sufficiently close to the observed values to make an initial assignment. Our final assignment is based on the agreement between observed and calculated relative intensities within the Zeeman patterns and the correct observation of 44 lines, which are listed in Table 2.

### Analysis of the Zeeman-splittings

The diagonal elements of the molecular  $g$ -tensor were obtained from the least squares fit to the

observed splittings. Because of the intermediate field case encountered here, their signs could be determined unambiguously [12]. The values for  $g_{aa}$ ,  $g_{bb}$  and  $g_{cc}$  are listed in Table 3 together with the anisotropies of the diagonal elements of the magnetic susceptibility tensor. Our data did not allow us to fit the second anisotropy ( $-\chi_{aa} + 2\chi_{bb} - \chi_{cc}$ ) with reasonable accuracy. This is due to the fact that the satellite frequencies in the observed transitions depend very little on its value. As a result the values of  $g_{aa}$ ,  $g_{bb}$  and  $g_{cc}$  as well as the value of  $(2\chi_{aa} - \chi_{bb} - \chi_{cc})$  remained essentially unchanged in the fit, if we restricted  $(2\chi_{bb} - \chi_{cc} - \chi_{aa})$  to be either equal to zero or to be equal to  $(2\chi_{aa} - \chi_{bb} - \chi_{cc})$ . For the final fit we set

$$(2\chi_{bb} - \chi_{cc} - \chi_{aa}) = (2\chi_{aa} - \chi_{bb} - \chi_{cc})$$

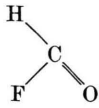
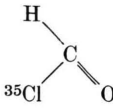
which is based on the observations made for HCOF.

### Discussion

Using the five Zeeman parameters determined here, the known  $r_s$ -structure [3] and an estimate of the bulk susceptibility as calculated from the Pascal constants [9] ( $\text{H} = -2.93$ ,  $\text{C} = -6.0$ ,  $\text{O} = +1.72$ ,  $\text{Cl} = -20.1$ ) the diagonal elements of the paramagnetic, diamagnetic, and total susceptibility tensors were calculated along with the second moments of the electronic charge distribu-



Table 3. Molecular parameters for Formylchloride as determined by microwave spectroscopy. For comparison the corresponding data for Formylfluoride are listed too.

			
Molecular $g$ -values <sup>a</sup>	$g_{aa}$	— 0.4227 (7)	— 0.5111 (48)
	$g_{bb}$	— 0.0771 (2)	— 0.0762 (51)
	$g_{cc}$	— 0.0371 (2)	— 0.0288 (36)
Molar magnetic susceptibility	$\frac{N_L(2\chi_{aa} - \chi_{bb} - \chi_{cc})}{10^{-6} \text{ erg/(G}^2 \text{ mole)}}$	6.1 (3)	4.1 (1.3)
anisotropies	$\frac{N_L(2\chi_{bb} - \chi_{aa} - \chi_{cc})}{10^{-6} \text{ erg/(G}^2 \text{ mole)}}$	5.9 (3)	4.1 <sup>b</sup>
Molar magnetic bulk susceptibility	$\frac{\frac{1}{3} N_L(\chi_{aa} + \chi_{bb} + \chi_{cc})}{10^{-6} \text{ erg/(G}^2 \text{ mole)}}$	—13.7	—27.3 (30) <sup>c</sup>
Rotational constants <sup>d</sup>	$A/\text{GHz}$	91.1536	77.96898
	$B/\text{GHz}$	11.7600	6.14079
	$C/\text{GHz}$	10.3968	5.68529
<sup>35</sup> Cl quadrupole coupling constants	$\chi_{aa}^{35\text{Cl}}/\text{MHz}$		—51.11 (5)
	$\chi_{bb}^{35\text{Cl}}/\text{MHz}$		30.20 (21)
	$\chi_{cc}^{35\text{Cl}}/\text{MHz}$		20.92 (21)

<sup>a</sup> The value of  $g_I = 0.54789$  was taken from Reference 12. The observed transitions were not affected by nuclear shielding.

<sup>b</sup> Not determined by observed splittings, but assumed equal to  $2\chi_{aa} - \chi_{bb} - \chi_{cc}$  in analogy to HCOF.

<sup>c</sup> Calculated from Pascal constants given in <sup>9</sup>). 10% uncertainty assumed.

<sup>d</sup> Taken from Reference [1] (HCOF) and Reference [2] (HCOCl).

tion and the electronic contribution to the inertial defect. The results are presented in Table 4. For comparison we have also included the values for the lighter homologue HCOF as determined by Flygare et al. [10].

It is seen, that the paramagnetic susceptibilities of HCOCl are nearly twice as big, as those of HCOF. Because both molecules have a very similar structure [3] and the same number of valence shell electrons this may then indicate, that HCOCl possesses a greater number of low lying excited electronic states (smaller energy differences in the denominator of the perturbation sum; see theoretical expression given in Table 4). To our knowledge no

photoelectron- or UV-spectroscopic study of HCOCl, which might be used to observe these states, has been made yet. We think, that the existence of such low energy states together with the bigger molecular electric quadrupole moment, which will cause a preorientation of reaction partners in the liquid phase and thus will lead to an increased “steric factor”, are important factors in determining the instability of HCOCl.

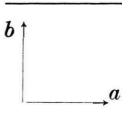
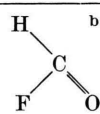
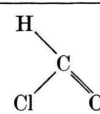
## Appendix

Nonvanishing matrixelements of the effective Hamiltonian used in this work. (For their derivation see for instance References [7] and [13].)

Diagonal elements:

$$\begin{aligned}
 \langle J, \tau, M_J, I, M_I | \mathcal{H}_{\text{rot}} | J, \tau, M_J, I, M_I \rangle &= h \{ A \langle J, \tau | J_a^2 | J, \tau \rangle + B \langle J, \tau | J_b^2 | J, \tau \rangle \\
 &\quad + C \langle J, \tau | J_c^2 | J, \tau \rangle \}, \\
 \langle J, \tau, M_J, I, M_I | \mathcal{H}_g^{\text{nuc}} | J, \tau, M_J, I, M_I \rangle &= -\mu_N (1 - \sigma) g_I^{35\text{Cl}} M_I H_z, \\
 \langle J, \tau, M_J, I, M_I | \mathcal{H}_g^{\text{mol}} | J, \tau, M_J, I, M_I \rangle &= -\mu_N \frac{M_J}{J(J+1)} \sum_{\gamma=a,b,c} g_{\gamma\gamma} \langle J, \tau | J_{\gamma}^2 | J, \tau \rangle H_z, \\
 \langle J, \tau, M_J, I, M_I | \mathcal{H}_{\chi} | J, \tau, M_J, I, M_I \rangle &= \frac{3M_J^2 - J(J+1)}{(2J-1)(2J+3)J(J+1)} \sum_{\gamma=a,b,c} \\
 &\quad \cdot (\chi - \chi_{\gamma\gamma}) \langle J, \tau | J_{\gamma}^2 | J, \tau \rangle H_z^2 - \frac{1}{2} \chi H_z^2,
 \end{aligned}$$

Table 4. Molecular parameters derived from the data presented in Table 3 and from the molecular structures.

			
Molecular quadrupole moment in units of $10^{-26}$ esu $\text{cm}^2$	$Q_{aa}$	— 4.5 (2)	— 7.6 (27)
$Q_{aa} = \frac{ e }{2} \left\{ \sum_n^{\text{nuclei}} (2a_n^2 - b_n^2 - c_n^2) - \langle 0   \sum_{\epsilon}^{\text{electrons}} (2a_{\epsilon}^2 - b_{\epsilon}^2 - c_{\epsilon}^2)   0 \rangle \right\}$ $= -\frac{\hbar  e }{16\pi^2 m_p} \left( \frac{2g_{aa}}{A} - \frac{g_{bb}}{B} - \frac{g_{cc}}{C} \right) - \frac{2mc^2}{ e } (2\chi_{aa} - \chi_{bb} - \chi_{cc})$	$Q_{bb}$	2.6 (2)	13.6 (57) <sup>a</sup>
	$Q_{cc}$	1.9 (4)	— 6.0 (63) <sup>a</sup>
Second moments of the nuclear charge distribution calculated from the geometry of the nuclear frame given in $\text{\AA}^2$	$\sum_n Z_n a_n^2$	20.94 (39)	40.84 (10)
	$\sum_n Z_n b_n^2$	3.88 (14)	4.42 (1)
	$\sum_n Z_n c_n^2$	0.0	0.0
Paramagnetic susceptibilities in units of $10^{-6}$ erg/(G <sup>2</sup> mole)	$\chi_{aa, \text{mole}}^p$	26.3 (6)	32.8 (2)
	$\chi_{bb, \text{mole}}^p$	102.8 (17)	199.8 (22)
	$\chi_{cc, \text{mole}}^p$	112.9 (17)	202.9 (18)
	$\chi_{aa, \text{mole}}^p = -\frac{N_L e^2}{2m^2 c^2} \sum_v^{\text{excited states}} \frac{ \langle 0   L_a   v \rangle ^2}{E_0 - E_v}$ $= -\frac{e^2}{4mc^2} \left\{ \frac{\hbar}{8\pi^2 m_p} \frac{g_{aa}}{A} - \sum_n^{\text{nuclei}} Z_n (b_n^2 + c_n^2) \right\} N_L$		
Diamagnetic susceptibilities in units of $10^{-6}$ erg/(G <sup>2</sup> mole)	$\chi_{aa, \text{mole}}^d$	— 38.0 (47)	— 58.6 (37)
	$\chi_{bb, \text{mole}}^d$	— 114.6 (58)	— 225.6 (69)
	$\chi_{cc, \text{mole}}^d$	— 130.6 (59)	— 232.8 (69)
	$\chi_{aa, \text{mole}}^d = -\frac{N_L e^2}{4mc^2} \langle 0   \sum_{\epsilon}^{\text{electrons}} (b_{\epsilon}^2 + c_{\epsilon}^2)   0 \rangle$ $= \chi_{aa, \text{mole}}^p - \chi_{aa, \text{mole}}^p$		
Second moments of the electronic charge distribution in $\text{\AA}^2$	$\langle 0   \sum_{\epsilon} a_{\epsilon}^2   0 \rangle$	24.4 (20)	47.1 (20)
	$\langle 0   \sum_{\epsilon} a_{\epsilon}^2   0 \rangle = -\frac{2mc^2}{e^2} (\chi_{bb} + \chi_{cc} - \chi_{aa})$ $-\frac{\hbar}{16\pi^2 m_p} \left( \frac{g_{bb}}{B} + \frac{g_{cc}}{C} - \frac{g_{aa}}{A} \right) + \sum_n^{\text{nuclei}} Z_n a_n^2$	$\langle 0   \sum_{\epsilon} b_{\epsilon}^2   0 \rangle$	7.6 (20)
	$\langle 0   \sum_{\epsilon} b_{\epsilon}^2   0 \rangle$	6.4 (20)	7.6 (20)
	$\langle 0   \sum_{\epsilon} c_{\epsilon}^2   0 \rangle$	2.6 (20)	6.1 (20)
Electronic contribution to the inertial defect [14] in amu $\text{\AA}^2$	$\Delta_{\text{elec}}$	— 0.0027	— 0.0039
	$\Delta_{\text{elec}} = -\frac{m}{m_p} (I_c g_{cc} - I_b g_{bb} - I_a g_{aa})$		

<sup>a</sup> calculated under assumption of an uncertainty of  $\pm 5 \cdot 10^{-6}$  erg/(G<sup>2</sup> mole) for the assumed value of 4.1 for  $(2\chi_{bb} - \chi_{cc} - \chi_{aa}) N_L$ .

<sup>b</sup> Data taken from Reference [10] and [[11]].

$$\langle J, \tau, M_J, I, M_I | \mathcal{H}_Q | J, \tau, M_J, I, M_I \rangle = \frac{1}{2} C_Q (J(J+1) - 3M_J^2) (I(I+1) - 3M_I^2).$$

Offdiagonal elements:

$$\langle J, \tau, M_J \pm 1, I, M_I \mp 1 | \mathcal{H}_Q | J, \tau, M_J, I, M_I \rangle = \frac{3}{4} C_Q (2M_J \pm 1)(2M_I \mp 1) \cdot \sqrt{(J \mp M_J)(J \pm M_J + 1)(I \pm M_I)(I \mp M_I + 1)},$$

$$\langle J, \tau, M_J \pm 2, I, M_I \mp 2 | \mathcal{H}_Q | J, \tau, M_J, I, M_I \rangle = \frac{3}{4} C_Q$$

$$\cdot \sqrt{(J \mp M_J)(J \mp M_J - 1)(J \pm M_J + 1)(J \pm M_J + 2)(I \pm M_I)(I \pm M_I - 1)(I \mp M_I + 1)(I \mp M_I + 2)}.$$

$A, B, C$  = rotational constants,

$$\mu_N = \frac{e\hbar}{2m_p c} = \text{nuclear magneton},$$

$\sigma$  = diamagnetic shielding at the  $^{35}\text{Cl}$  nucleus,

$g_I^{^{35}\text{Cl}}$  =  $g$ -value of the  $^{35}\text{Cl}$  nucleus,

$H_z$  = magnetic field strength,

$g_{\gamma\gamma}$  = diagonal elements of the molecular  $g$ -tensor,

$\chi_{\gamma\gamma}$  = diagonal elements of the susceptibility tensor,

$\chi$  =  $(\chi_{aa} + \chi_{bb} + \chi_{cc})/3$  bulk susceptibility.

$\langle J, \tau \| J_{\gamma^2} \| J, \tau \rangle$  = reduced matrix element for the square of the angular momentum operators in the asymmetric top basis,

$$C_Q = \frac{h}{J(2J-1)I(2I-1)} \cdot \left\{ \sum_{\gamma} \chi_{\gamma\gamma}^{^{35}\text{Cl}} \frac{\langle J, \tau \| J_{\gamma^2} \| J, \tau \rangle}{(J+1)(2J+3)} \right\},$$

$\chi_{\gamma\gamma}^{^{35}\text{Cl}}$  = quadrupole coupling constants for the  $^{35}\text{Cl}$  nucleus.

### Acknowledgement

Dem Fonds der Chemischen Industrie sei für die Gewährung eines Promotionsstipendiums (K.-F. Dössel), der Deutschen Forschungsgemeinschaft für die Bereitstellung von Sach- und Personalmitteln gedankt. Die erforderlichen Rechnungen wurden auf der PDP-10 Anlage im Rechenzentrum der Universität durchgeführt. Herrn Prof. Dr. H. Dreizler danken wir für die Durchsicht des Manuskripts.

- [1] O. H. Leblanc, W. W. Laurie, and W. D. Gwinn, *J. Chem. Phys.* **33**, 598 (1960).
- [2] F. C. Hisatsune and J. Heicklen, *Can. J. Spectrosc.* **18**, 77 (1973).
- [3] H. Takeo and C. Matsumura, *J. Chem. Phys.* **64**, 4536 (1976).
- [4] D. H. Sutter, *Z. Naturforsch.* **26a**, 1644 (1971).
- [5] D. H. Sutter and W. H. Flygare, The Molecular Zeeman Effect, in *Topics in Current Chemistry*, Vol. 63, 89–196 (1976).
- [6] H. D. Rudolph, *Z. Naturforsch.* **23a**, 540 (1968).
- [7] W. Hüttner and W. H. Flygare, *J. Chem. Phys.* **47**, 4137 (1967).
- [8] E. Hamer, Thesis, Kiel 1973.
- [9] H. F. Hameka, *Advanced Quantum Chemistry*, Addison-Wesley Publ. Co., Reading 1965, Massachusetts, p. 180.
- [10] S. L. Rock, J. K. Hancock, and W. H. Flygare, *J. Chem. Phys.* **54**, 3450 (1971).
- [11] A. Guanieri et al., *Boll. Sci. Fac. Chim. Ind. Bologna* **20**, 105 (1962).
- [12] See Ref. [5], p. 146 and M. Suzuki and A. Guarnieri, *Z. Naturforsch.* **30a**, 497 (1975).
- [13] C. H. Townes and A. L. Schawlow, *Microwave Spectroscopy*, McGraw-Hill, Inc., New York 1956.
- [14] T. Oka and Y. Morino, *J. Mol. Spectry.* **6**, 472 (1961).